Acta Crystallographica Section D
Biological Crystallography
ISSN 0907-4449

Dynamic response of tetragonal lysozyme crystals to changes in relative humidity: implications for post-growth crystal treatments

I. Dobrianov,[a] S. Kriminski,[a] C. L. Caylor,[a] S. G. Lemay,[a] C. Kimmer,[a] A. Kisselev,[a] K. D. Finkelstein[b] and R. E. Thorne[a]*

[a]Laboratory of Atomic and Solid State Physics, Cornell University, Ithaca, NY 14853, USA, and [b]Cornell High-Energy Synchrotron Source (CHESS), Ithaca, NY 14853, USA

Correspondence e-mail: ret6@cornell.edu

Received 17 July 2000
Accepted 17 October 2000

The dynamic response of tetragonal lysozyme crystals to dehydration has been characterized *in situ* using a combination of X-ray topography, high-resolution diffraction lineshape measurements and conventional crystallographic diffraction. For dehydration from 98% relative humidity (r.h.) to above 89%, mosaicity and diffraction resolution show little change and X-ray topographs remain featureless. Lattice constants decrease rapidly but the lattice-constant distribution within the crystal remains very narrow, indicating that water concentration gradients remain very small. Near 88% r.h., the *c*-axis lattice parameter decreases abruptly, the steady-state mosaicity and diffraction resolution degrade sharply and topographs develop extensive contrast. This transformation exhibits metastability and hysteresis. At fixed r.h. < 88% it is irreversible, but the original order can be almost completely restored by rehydration. These results suggest that this transformation is a first-order structural transition involving an abrupt loss of crystal water. The front between transformed and untransformed regions may propagate inward from the crystal surface and the resulting stresses along the front may degrade mosaicity. Differences in crystal size, shape and initial perfection may produce the observed variations in degradation timescale. Consequently, the success of more general post-growth treatments may often involve identifying procedures that either avoid lattice transitions, minimize disorder created during such transitions or maintain the lattice in an ordered metastable state.

1. Introduction

Water plays a central role in maintaining the structure and activity of protein molecules both in solution and in the crystalline form (Rupley & Careri, 1991; Frey, 1994). The effects of water removal (dehydration) on protein crystals have been extensively studied both from a crystallographer's viewpoint, focusing on changes in lattice structure, in molecular conformation and in the arrangement of surrounding water molecules (Crowfoot *et al.*, 1937; Perutz, 1946, 1954; Boyes-Watson *et al.*, 1947; Huxley & Kendrew, 1953; Einstein & Low, 1962; Salunke *et al.*, 1985; Kodandapani *et al.*, 1990; Kachalova *et al.*, 1991; Nagendra *et al.*, 1998), as well as from a physico-chemical viewpoint, focusing on fundamental crystal properties including hydration, Young's modulus and relaxation times (Khatchaturyan, 1977; Morozov & Morozova, 1981; Gevorkyan & Morozov, 1983; Morozov *et al.*, 1985, 1988).

Studies of dehydration of tetragonal lysozyme crystals (Salunke *et al.*, 1985; Morozov *et al.*, 1985, 1988; Kodandapani *et al.*, 1990) have found that steady-state lattice parameters decrease and Young's modulus increases with decreasing

relative humidity (r.h.). Between 90 and 93% r.h. the lattice parameters decrease by ∼1% in all directions and this decrease has been considered as evidence for a lattice transition (Salunke *et al.*, 1985; Kodandapani *et al.*, 1990). Dehydration to 88% r.h. produces a translation (0.64, 0.33, 0.03 Å) and rotation (0.8°) of the asymmetric unit and a conformational change involving a 0.21 Å r.m.s. deviation of the main chain relative to the native structure at ∼98% r.h. (Kodandapani *et al.*, 1990). For a r.h. of 84% and below, the steady-state diffraction resolution degrades substantially and this degradation is reversible upon rehydration (Salunke *et al.*, 1985). Abrupt changes in lattice constants at well defined relative humidities have been observed for many other proteins (Perutz, 1946; Huxley & Kendrew, 1953; Einstein & Low, 1962; Salunke *et al.*, 1985) and are likely to be a generic feature of macromolecular crystals. Abrupt degradation of diffraction properties has also been observed, although some crystal forms of some proteins show improved diffraction resolution upon dehydration.

Aside from its fundamental interest, the process of dehydration shares many features with post-growth treatments such as substrate or drug binding, heavy-atom compound binding and cryoprotectant soaks. All involve diffusive transport within the crystal; they often cause changes in lattice constant, lattice symmetry and molecular conformation that lead to lattice stresses, crystal cracking and mosaic broadening; they also usually degrade (but occasionally improve) crystal *B* factors and diffraction resolution. These similarities suggest that controlled dehydration can serve as a simple model for studying effects of post-growth treatments on crystal order.

We have used a combination of X-ray diffraction techniques to study the dynamic evolution of lattice parameters and lattice order during dehydration of tetragonal lysozyme crystals. Near 88% r.h., the *c*-axis lattice constant abruptly changes by ∼9% and the diffraction resolution and mosaicity degrade dramatically. For dehydrations to near 88% r.h., the time required for degradation of diffraction resolution can vary by orders of magnitude and can be far longer than the characteristic time required for vapor-pressure equilibration. This suggests that the lattice can remain in a metastable state and that the lattice transition that occurs near 88% r.h. is first order. Patterns of disorder visible in X-ray images of dehydrated crystals suggest that mosaic broadening may result from lattice stresses occurring as the front separating transformed and untransformed regions propagates inward from the crystal surface. These results provide insight into how the lattice relaxes as water is removed and have consequences for the understanding of more general post-growth crystal treatments.

2. Materials and methods

Tetragonal hen egg-white lysozyme crystals were grown at room temperature (∼295 K) in 0.1 *M* acetate buffer at pH 4.5 from solutions containing either 0.48 *M* NaCl and 90 mg ml^{-1} lysozyme (Seikagaku, 6× recrystallized) or 0.75 *M* NaCl and 25 mg ml^{-1} lysozyme. The equilibrium relative humidities corresponding to these mother liquors are approximately 98 and 97%, respectively. Typical NaCl concentrations used in lysozyme crystal-growth experiments correspond to 95–99% r.h.

Crystals for steady-state dehydration measurements were placed together with a plug of saturated salt solution in X-ray capillaries and the capillaries were then sealed with grease. A few salt crystals added to the plug solution ensured that it remained saturated; in any case, solution dilution owing to water removal from the crystal was negligible. Equilibrium relative humidities between 97 and 75% at T = 295 K were obtained using potassium nitrate (93.5%), zinc sulfate (89%), sodium benzoate (88%), potassium chromate (87.5%), potassium chloride (86%), potassium bromide (83.5%), ammonium sulfate (79%) and sodium chloride (75%) (Rockland, 1960). The crystal-to-salt solution distance was ∼1 cm. Crystals were equilibrated for several days to several weeks prior to measurement.

Crystals for time-resolved measurements were initially sealed in capillaries together with a plug of mother liquor. Immediately prior to measurement, the grease at one end was removed, the mother liquor and as much of the remaining liquid surrounding the crystal as possible was wicked away, a salt-solution plug was injected and the capillary was then resealed. The typical time from injection of salt solution (*i.e.* the start of dehydration) to the first diffraction measurements was ∼6 min, with a comparable uncertainty.

X-ray diffraction patterns and topographs were measured *in situ* during dehydration at $T = 295 \pm 1$ K at the Cornell High-Energy Synchrotron Source (CHESS) on stations B-2 and C-2 using $\lambda \simeq 1.24$ Å X-rays. Partial crystallographic data sets consisting of 4 or 6° oscillations about two perpendicular orientations were collected using image plates. *SCALEPACK*, *DENZO* and subroutines from the *CCP*4 package (Collaborative Computational Project, Number 4, 1994) were used to index and scale the diffraction patterns and to determine lattice constants, *B* factors, diffraction resolutions and mosaicity parameters. X-ray topographs (Tanner, 1976; Fourme *et al.*, 1995, 1999; Izumi *et al.*, 1996; Stojanoff *et al.*, 1997; Dobrianov *et al.*, 1998, 1999; Otalora *et al.*, 1999; Vidal *et al.*, 1999) were recorded using Kodak Industrex SR film held ∼4 cm from the crystal. Topographs are images of a crystal formed by a single diffraction spot when the crystal is illuminated using an unfocussed highly parallel X-ray beam. Image contrast arises from variations in the strength of diffraction from point to point within the crystal associated with variations in lattice orientation, spacing and short-range order (*i.e.* *B*-factor variations.) Topographs were acquired in ∼1 min and partial diffraction data sets in ∼10 min, times that were short compared with those for the crystal's response during dehydration.

High-resolution θ–2θ and mosaic scans through selected reflections were performed during dehydration on CHESS station C-2 using a Huber six-circle diffractometer and Si (111) monochromator and analyzer crystals. The X-ray beam illuminated the entire crystal so that these scans measured the

distributions of lattice-plane spacings and lattice orientations within the crystal, respectively. The time required for each scan was ∼1.5 min. Because of rapid peak motion during dehydration, frequent crystal reorientation was required to remain on the peak. For dehydration to 88% r.h. and below, the decay of peak intensities after the lattice transition restricted data collection to earlier times.

To supplement measurements at CHESS, additional steady-state and time-resolved diffraction measurements (with much coarser time resolution) were performed using a Bruker rotating-anode source. Diffraction patterns were recorded using a SMART 1k × 1k CCD system and were indexed and analyzed using the programs *SMART* and *SAINT*. The diffraction resolution (for $I/\sigma > 2$) obtained from undehydrated crystals was ∼1.9 Å using the rotating-anode source and ≤1.5 Å at CHESS. In all, more than 100 crystals were characterized.

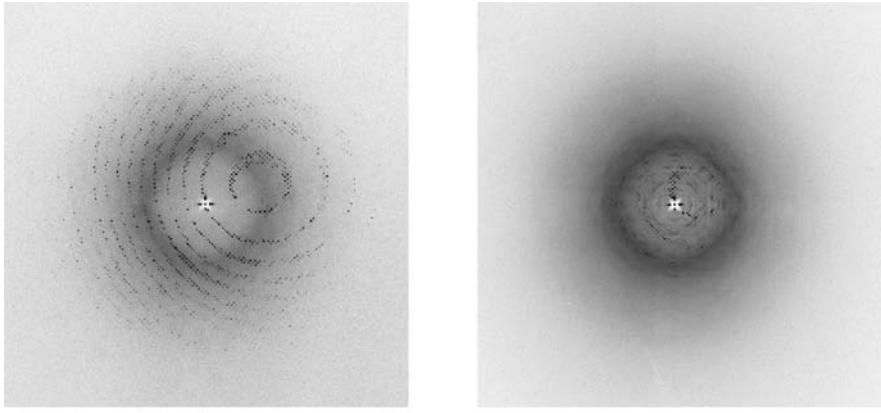

Figure 1
Diffraction pattern of tetragonal lysozyme (*a*) 5 min and (*b*) 2 h 36 min after the start of dehydration from 98 to 86% r.h. Each pattern records a 2° oscillation. The calculated diffraction resolutions ($I/\sigma = 2$) and mosaicity parameters are (*a*) 1.6 Å and 0.06° and (*b*) 3.7 Å and 1.9°.

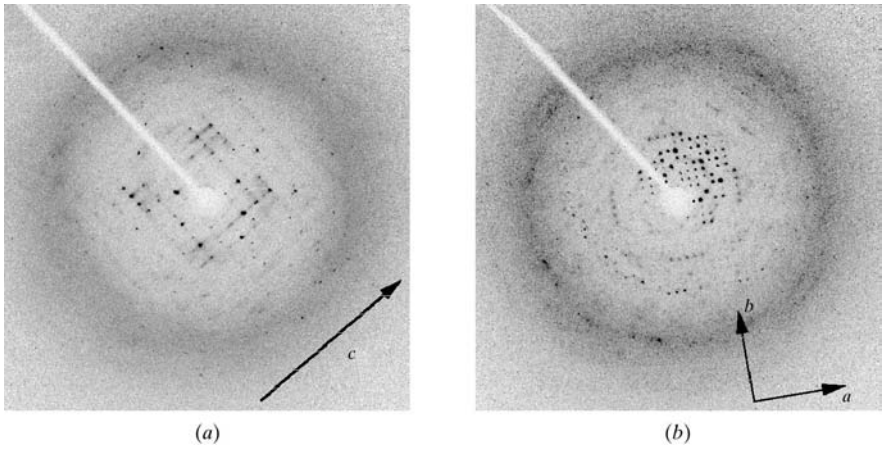

Figure 2
Fixed-orientation diffraction patterns for a degraded lysozyme crystal dehydrated to 86% r.h., with the fourfold *c* axis oriented (*a*) perpendicular and (*b*) parallel to the incident beam direction.

3. Experimental results

Consistent with earlier work, steady-state lattice parameters decrease gradually with decreasing r.h. for r.h. ≥ 93% and then decrease rapidly (by ∼1.5% in *a* and ∼1.2% in *c*) between 93 and 88% r.h. For dehydration to >88% r.h., the diffraction resolution and mosaicity do not change and X-ray topographs do not develop appreciable contrast. We do not observe evidence for a previously proposed lattice transition between 93 and 90% r.h. (Salunke *et al.*, 1985; Kodandapani *et al.*, 1990), but instead find a continuous lattice-parameter variation there. For dehydration to r.h. < 88%, essentially all crystals show dramatically degraded diffraction resolution and mosaicity (usually such that their diffraction patterns could not be indexed) and their topographs develop extensive and complex contrast, providing evidence for a different lattice transition. Systematic studies were performed at $T \simeq 295$ K for dehydration to r.h.s of 83.5, 86, 87.5, 88 and 89%, below and in the vicinity of this disordering lattice transition.

3.1. General features of steady-state and time-dependent properties

Fig. 1 shows diffraction patterns acquired immediately after and 2 h 36 min after the start of dehydration to 86% r.h. The diffraction pattern and diffraction resolution show little change until the lattice parameters have decreased below the steady-state values corresponding to r.h. ≃ 88%; they then degrade rapidly and dramatically. This degradation – from a resolution of <2 to >4 Å – typically occurs in ∼30 min (and in as little as 5 min) and begins ∼1–4 h after dehydration to 86% r.h. is initiated. For dehydration to ≤83.5% r.h., the lattice parameters decrease more rapidly, the diffraction resolution degrades sooner and once it begins degradation occurs more rapidly, as expected. As shown in Fig. 2, the diffraction resolution degradation is accompanied by a large increase in diffuse scattering. Strong diffuse streaks are observed when the fourfold (*c*) axis is perpendicular to the incident beam, whereas very weak diffuse streaks are observed when the *c* axis is parallel to the beam. This anisotropy suggests that the disorder responsible is greatest along the *c* axis, which may be related to the smaller number of intermolecular contacts along this direction (Blake *et al.*, 1965; Kodandapani *et al.*, 1990; Nadarajah & Pusey, 1996).

Fig. 3 shows the lattice parameter a and diffraction resolution ($I/\sigma = 2$) as a function of time during dehydration to 86% r.h. for several samples varying in volume from ~0.1 to 1 mm^3. The time for the lattice parameters to evolve and for the diffraction resolution to degrade increases with increasing crystal volume and thus decreasing surface-to-volume ratio. The characteristic time for the resolution to degrade to 3 Å ranges from <1 h for 0.1 mm^3 crystals to >4 h for 1 mm^3 crystals, roughly consistent with numerical estimates for diffusive equilibration between the crystal and salt solution (Fowlis *et al.*, 1988; Morozov *et al.*, 1995).

Fig. 4 shows the trajectory of lattice parameter a *versus* lattice parameter c that occurs during dehydration to 86% r.h., using the data for the crystals of various sizes in Fig. 3. Despite the large difference in dehydration rates, the lattice parameters for crystals of different sizes follow a single trajectory. The variation is strongly non-linear, suggesting different regimes of lattice deformation and/or molecular conformation as water removal proceeds. Steady-state values of the lattice parameters usually could not be obtained because the diffraction resolution degraded so that diffraction patterns could not be indexed.

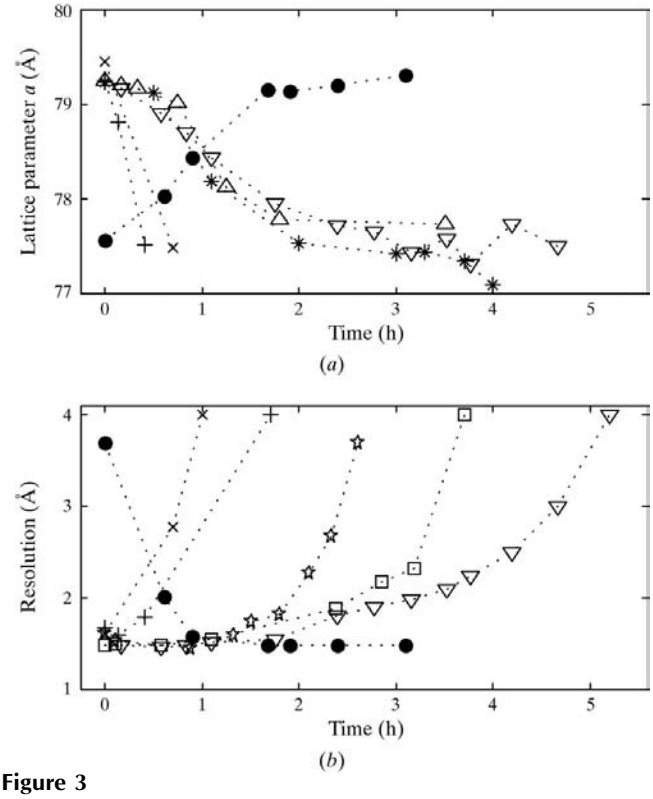

Figure 3
(*a*) Lattice parameter a and (*b*) diffraction resolution ($I/\sigma = 2$) *versus* time for several crystals of different volumes dehydrating to 86% r.h. The approximate sample volumes (in mm^3) are 0.10 (crosses), 0.20 (plus signs), 0.22 (triangles), 0.32 (squares), 0.35 (stars), 0.5 (asterisks) and 1.0 (inverted triangles). The filled circles are data for rehydration of the 0.35 mm^3 sample back to 98% r.h. The effective dehydration start time is uncertain by ~20 min, primarily because of variations in the amount of mother liquor remaining trapped between the crystal and capillary wall after sample preparation.

Fig. 5 shows the steady-state relation between lattice parameter a and lattice parameter c for dehydration to between 98% and 87% r.h. 'Steady-state' values were determined at least 1 d after the start of dehydration, much longer than the timescale of the response evident in Fig. 4. The upper solid line passing through this data is the same as that in Fig. 4. Consequently, the *steady-state* lattice parameters for dehydration to r.h. > 87% fall on the lattice-parameter trajectory *in time* during dehydration to r.h. < 87%. For dehydration to 88% r.h. and below, diffraction resolution usually degraded so that 'steady-state' diffraction patterns as defined above could

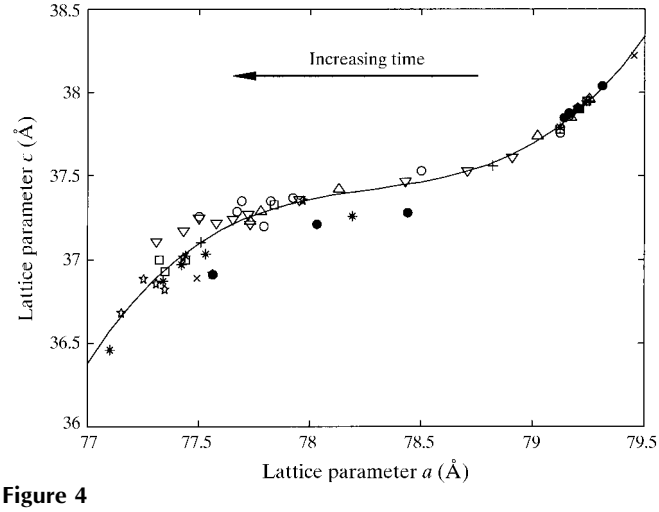

Figure 4
Lattice parameter c *versus* lattice parameter a during dehydration to 86% r.h. for samples of different volumes. The samples and symbols are the same as in Fig. 3. The solid line is a guide to the eye. The absolute changes in a and c over the humidity range shown are comparable, but the change in c per lysozyme molecule is much larger.

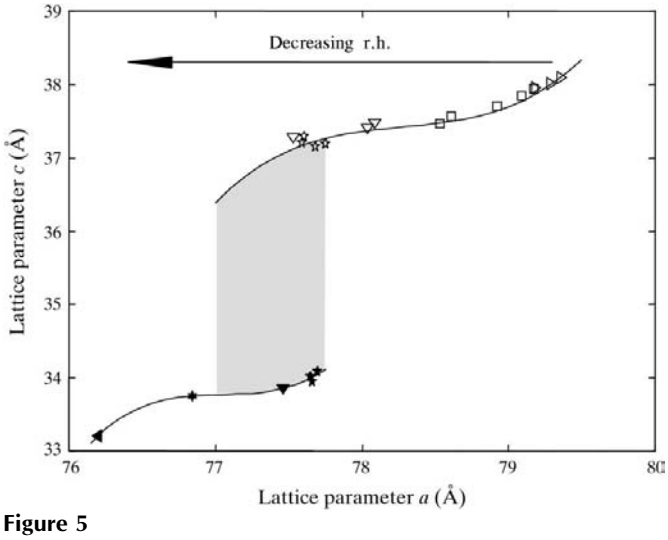

Figure 5
Lattice parameter c *versus* lattice parameter a measured at least 1 d after the start of dehydration (or at an intermediate time at which the diffraction resolution still allowed reflection indexing) during dehydration to 98 (right-pointing triangle), 93 (square), 88 (five-pointed star), 87 (inverted triangle), 83 (left-pointing triangle) and 79% (six-pointed star). The open symbols correspond to crystals with diffraction resolution <3 Å and the solid symbols to those with resolution >3 Å. The upper solid line is the same as in Fig. 4; the lower solid line is a guide to the eye.

not be indexed. However, at intermediate times following the onset of resolution degradation indexing was sometimes possible and the lattice parameters thus obtained fall on the lower curve in Fig. 5. These data indicate that resolution degradation coincides with a discontinuous ~3 Å or 9% decrease in *c*, although no discontinuity is observed in *a*. The size of this discontinuity suggests that the transition near 88% r.h. may involve the cooperative loss of two layers of water molecules running normal to *c*, although a large change in lysozyme conformation cannot be ruled out since the resolution was not sufficient for a structure determination. Note that the upper solid line in Fig. 5 corresponding to the trajectory in Fig. 4 followed during dehydration to 86% r.h. extends to lower *a* and *c* values than can be obtained in the steady state. Consequently, the trajectory in time must exhibit hysteresis (schematically illustrated by the shaded region) and the lattice states with $a < 77.5$ Å and $c > 36$ Å in Fig. 4 must be metastable.

Fig. 6 shows a time series of θ–2θ scans acquired using a single diffraction peak at $2\theta \simeq 13^\circ$ from a crystal dehydrating to 86% r.h. The acquisition time for each scan was ~1.5 min and the scans range from $t = 3$ h 30 min to $t = 3$ h 54 min after the start of dehydration, just before the diffraction resolution of this sample began to rapidly degrade. The peak full-width-at-half-maximum (FWHM) is roughly $\Delta(2\theta) \simeq 0.009^\circ$. The broadening arising from peak motion during each scan is ~0.003° and the instrumental resolution was $\Delta Q/Q \simeq 3 \times 10^{-4}$ or $\Delta(2\theta)_{\rm IR} \simeq 0.004^\circ$. The observed FWHM thus indicates a slight intrinsic broadening corresponding to a lattice-constant spread within the crystal of <0.03% or roughly 1/100 of the lattice-constant change from 98 to 88% r.h. Consequently, large lattice strains and thus large water concentration gradients do not develop during the portion of dehydration examined. This suggests that the dehydration rate is not limited by water transport within the crystal. The presence of larger strains existing within a small fraction of the crystal volume cannot be ruled out as these would contribute only to the poorly resolved wings of the peaks. The development of large strains as the diffraction resolution degrades also cannot be ruled out, since locating peaks and measuring their intensities using our high-resolution configuration became difficult.

Fig. 7 shows examples of steady-state X-ray topographs. For dehydration above 88% r.h., the topographs show little contrast aside from some evidence of overall crystal bending. This bending may be a consequence of non-uniform dehydration-induced stresses associated with the irregular crystal shapes that result in vapour-diffusion growth and/or from the contact of one crystal face with the capillary wall. For dehydration below 88% (Figs. 7*c*–7*f*), topographs show extensive contrast with a symmetry consistent with a crystal 'drying out' They usually also show evidence of cracks and dislocations. For r.h. $\leq$ 79% these defects can form dense interconnected webs, as shown in Fig. 7(*f*) (and as was inadvertently observed by Stojanoff & Siddons, 1996). The cracks often run perpendicular to *c,* consistent with recent observa-

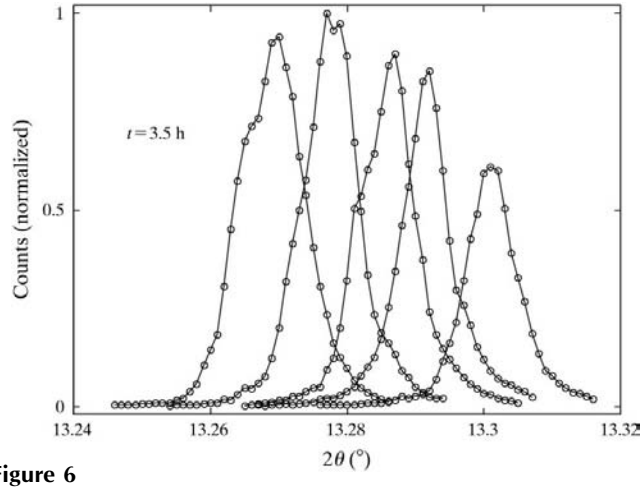

Figure 6
Time series of θ–2θ scans acquired using a single diffraction peak at $2\theta \simeq 13^\circ$ from a crystal dehydrating to 86% r.h. The time required to acquire each scan was ~1.5 min and the data range from $t = 3$ h 30 min to $t = 3$ h 54 min after the start of dehydration.

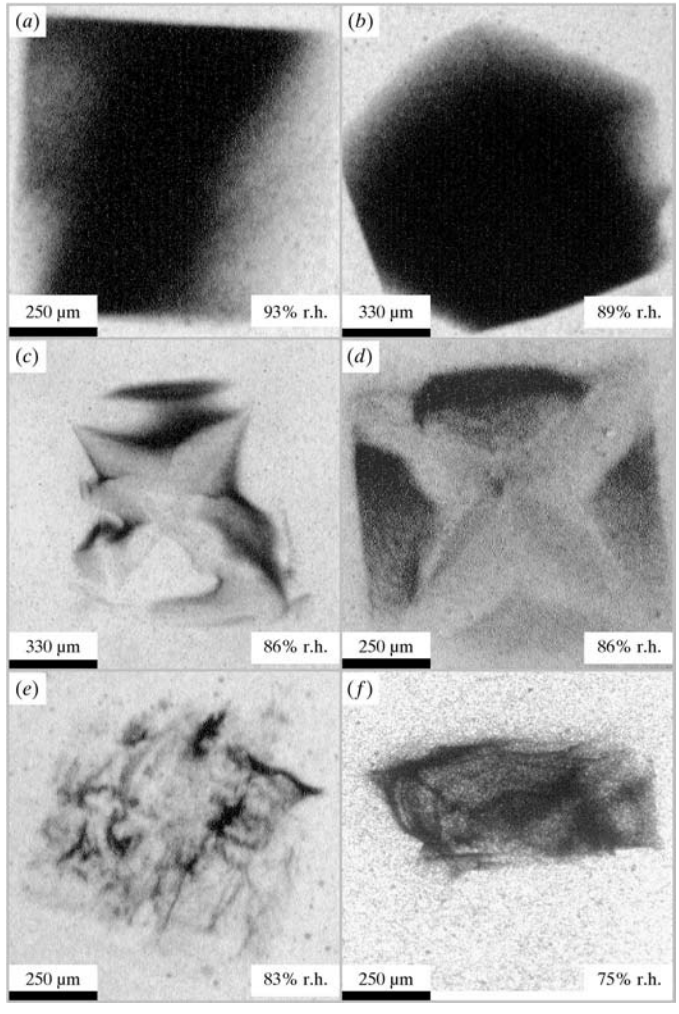

Figure 7
X-ray topographs of crystals dehydrated to (*a*) 93, (*b*) 89, (*c*) 86, (*d*) 86, (*e*) 83 and (*f*) 75%, acquired in steady-state long after the start of dehydration.

tions of lysozyme crystals immersed in hypotonic and hypertonic solutions (Garcia-Ruiz *et al.*, 2000).

Fig. 8 shows a time series of X-ray topographs for a crystal dehydrating to 83.5% r.h. Comparison with diffraction patterns shows that topographs develop significant contrast (*e.g.* as in Fig. 9*c*) once the diffraction resolution begins to degrade. The development of contrast also coincides with an increase in mosaic spread: mosaicity parameters (as deduced using *DENZO*) increase from hundredths of a degree before to 1° or more after the resolution degrades. Image contrast may thus result from variations in lattice orientation or mosaicity or from variations in the integrated strength of ordered diffraction (corresponding to spatial variations in crystal *B* factors).

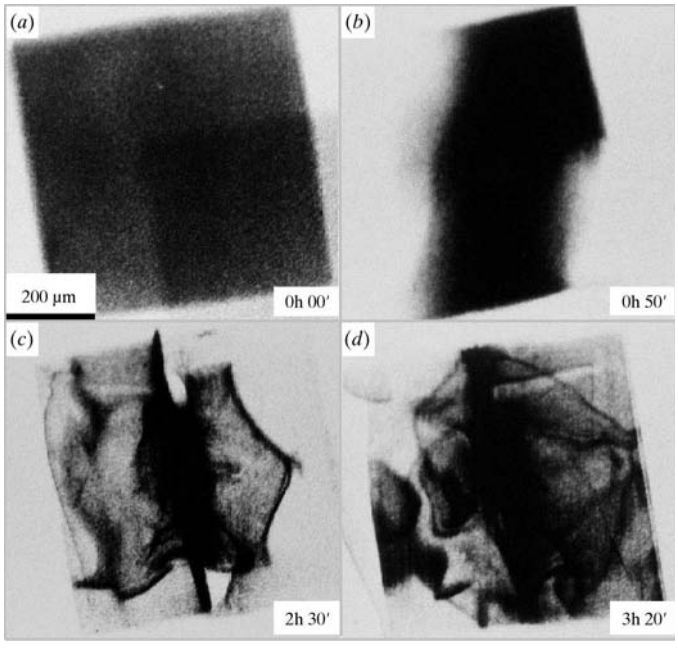

Figure 8
Time series of X-ray topographs for a crystal dehydrating to 83.5% r.h.

3.2. Dehydration near the lattice transition

For dehydration of crystals of similar size to 87–89% r.h. (near the r.h. of the lattice transition), the time required from the start of dehydration until the lattice transition occurs shows significant crystal-to-crystal variability. Because of the broad range of timescales, most measurements in this r.h. range were performed using a laboratory X-ray source.

For dehydration to 87.5% r.h., 16 out of 20 samples had substantially degraded diffraction resolution (>4.5 Å) at the time of first measurement, which ranged from 1 to 4 d after dehydration began. However, two crystals continued to diffract well (<2.5 Å) 12 and 80 d after preparation, respectively. Two others diffracted well (<2.5 Å) after 5 d but had degraded to >4.5 Å after 10 d. For dehydration to 89% r.h., the behavior was essentially reversed. Of 14 crystals studied, 12 continued to diffract well (<2.5 Å) for as long as they were measured (from 4 to 80 d) and two that diffracted well after 2 d had degraded to >4.5 Å after 80 d. In no case did a crystal that diffracted poorly subsequently recover. Thus, the timescale on which the diffraction degrades can exceed by one to three orders of magnitude the time (a few hours) for nominal equilibration of the crystal's water content with the salt solution. This implies that the lattice can remain in a metastable ordered state for extended periods before irreversibly (and often rapidly) degrading. This metastability together with the discontinuity and hysteresis of the *c* lattice parameters suggest that the lattice undergoes a structural phase transition at ∼88% r.h.

Although metastability is to be expected given the abrupt nature of the transition, temperature variations could also cause irreproducible behavior either by changing the salt solution's r.h. or by directly affecting the molecules or crystal lattice. Over the course of several days from the start of dehydration to the completion of diffraction measurements temperature variations as large as ±2 K at CHESS and ±1 K for crystals measured using the laboratory source may have occurred. However, irreproducibility is observed for crystals mounted, stored and measured together and the pattern of

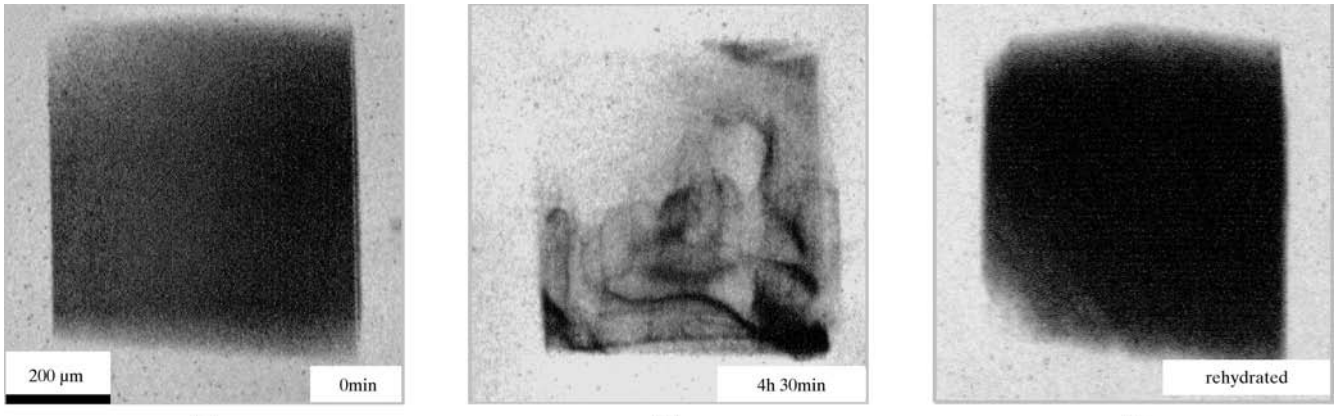

Figure 9
X-ray topographs of a crystal (*a*) before dehydration, (*b*) after dehydration to 83.5% r.h. and (*c*) 8 h after the start of rehydration to 98% r.h.

irreproducibility is not obviously consistent with temperature variations.

3.3. Reversibility

Although crystals whose diffraction properties are degraded by dehydration to <88% do not spontaneously recover, rehydration above the transition at 88% r.h. can almost completely restore original order. For example, crystals with severely degraded diffraction resolution (>5 Å) and mosaicity parameter (>1°) recover to ∼1.5 Å and <0.1° when rehydrated to 93.5% r.h.; the timescale for this recovery is comparable to that for dehydration (∼1 h), as shown in Fig. 3(*b*). As shown in Fig. 9, most contrast visible in topographs disappears upon rehydration, consistent with the restoration of mosaicity and resolution. As shown in Fig. 3(*a*), the lattice parameters appear to follow a slightly different trajectory than during dehydration, although this may reflect inhomogeneous recovery within the crystal.

4. Discussion

The present results provide a detailed picture of how the lattice constants and lattice order of tetragonal lysozyme crystals evolve during dehydration. Significant dehydration and lattice contraction (Δa, $\Delta c > 2\%$) can occur with no deleterious effects on crystal diffraction properties. However, beyond a critical r.h. of ∼88% (at $T \simeq 294$ K), the lattice undergoes a transition involving a large change in *c*-axis lattice parameter that dramatically degrades crystal diffraction resolution and mosaicity and increases diffuse scatter. Well below this r.h. the transition occurs rapidly. However, near the critical r.h. the lattice can remain in an ordered metastable state for extremely long times compared with those required for r.h. equilibration before decaying in a relatively short time to the disordered state. These general features are characteristic of a first-order phase transition.

The detailed nature of the disordered state is uncertain because it shows little ordered diffraction from which information about molecular changes might be derived. However, the large change in *c*-axis lattice parameter together with the observed diffuse streaks suggest that random displacements or conformation changes possibly associated with water loss in planes normal to this axis may dominate this disorder.

The absence of a significant lattice-constant spread (*i.e.* significant strain) during dehydration prior to the lattice transition suggests that appreciable gradients in water content do not develop within the crystal even though the lattice constants shrink by ∼2% in ∼1 h. This absence of gradients is consistent with estimates and measurements of diffusive water transport within the crystal (Fowlis *et al.*, 1988; Morozov *et al.*, 1995) and is consistent with the absence of significant mosaic broadening and contrast in X-ray topographs before the lattice transition. The mosaic broadening and image contrast that develop once the diffraction resolution begins to degrade are thus likely to be associated with the lattice transition.

The apparent first-order character of the lattice transition near 88% r.h. has consequences for how mosaic disorder and topographic contrast may arise. Such transitions are typically characterized by nucleation phenomena, in which a region of the new phase must form to 'seed' the transformation of the bulk. In the present case, the constraints of the surrounding lattice are likely to provide a significant barrier to the molecular displacements, rotations and/or conformation changes associated with the transition. Nucleation and lattice relaxation is likely to first occur where lattice constraints are less severe, such as at the crystal surface (especially at facet edges and corners) and perhaps also at internal defects like cracks and dislocations. The large timescale variations observed near 88% r.h. may reflect the statistics of the nucleation process, differences in crystal shape or size or differences in initial crystal perfection. Once nucleation occurs, a 'front' separating transformed and untransformed regions may propagate inward to the crystal center. Because of the transition's large *c*-axis lattice change, large stresses are likely to develop along this front, driving formation of dislocations, cracks and other defects responsible for the mosaic broadening. Evidence for such front propagation is provided by X-ray topographs, both from the general shape of the contrast patterns (Fig. 7) and from the common observation that during the transition the diffracted intensity fades out first in the outer regions of the crystal (as in Fig. 8*c*), suggesting that these regions transform first. After the transformation, residual diffraction is often only observed in ribbon-like regions which we interpret as cracks. Relaxation of lattice constraints in the vicinity of cracks may thus facilitate lattice relaxation and reduce disorder.

5. Implications for post-growth crystal treatments

Controlled dehydration shares many features with other post-growth treatments including heavy-atom and cryoprotectant soaks and drug binding. The present results demonstrate useful diffraction techniques for studying how these treatments create disorder. X-ray topography should be particularly useful for characterizing spatial non-uniformities of lattice relaxation within the crystal and their effects on mosaicity and resolution.

The results for lysozyme dehydration to >88% r.h. suggest that treatments of other macromolecular crystals involving small molecules (*e.g.* heavy-atom compounds, cryoprotectants, drugs) need not create additional disorder even when the overall change in lattice parameter is large, provided that the lattice parameters evolve continuously and that the treatment is performed gradually enough for diffusive equilibrium within the crystal to be approximately maintained. However, if a treatment causes a discontinuous change in lattice parameter, then the motion of the resulting phase boundary through the crystal will be likely to create dislocations, cracks and other defects that may significantly degrade mosaicity and diffraction resolution. As in dehydration, structural metastability conferred by the constraints of the crystal lattice may allow metastable order to be maintained in initially highly perfect

crystals if the treatment is performed sufficiently gradually. Consequently, the success of more general post-growth treatments may often involve identifying procedures that either avoid lattice transitions, minimize disorder created during such transitions or that maintain the lattice in an ordered metastable state.

We wish to thank to A. Chernov and G. DeTitta for fruitful discussions and M. Brink for technical assistance. This work was supported by NASA (NAG8-1357).

References

Blake, C. C. F., Koenig, D. F., Mair, G. A., North, A. C. T., Phillips, D. C. & Sarma, V. R. (1965). *Nature (London)*, **206**, 757–761.
Boyes-Watson, J., Davidson, E. & Perutz, M. F. (1947). *Proc. R. Soc. London Ser. A*, **191**, 83–132.
Collaborative Computational Project, Number 4 (1994). *Acta Cryst.* D**50**, 760–763.
Crowfoot, D., Riley, D., Bernal, J. D., Fankuchen, I. & Perutz, M. (1937). *Nature (London)*, **141**, 521–524.
Dobrianov, I., Caylor, C., Lemay, S. G., Finkelstein, K. D. & Thorne, R. E. (1999). *J. Cryst. Growth*, **196**, 511–523.
Dobrianov, I., Finkelstein, K. D., Lemay, S. G. & Thorne, R. E. (1998). *Acta Cryst.* D**54**, 922–937.
Einstein, J. R. & Low, B. W. (1962). *Acta Cryst.* **15**, 32–34.
Fourme, R., Ducruix, A., Ries-Kautt, M. & Capelle, B. (1995). *J. Synchrotron Rad.* **2**, 136–142.
Fourme, R., Ducruix, A., Ries-Kautt, M. & Capelle, B. (1999). *J. Cryst. Growth*, **196**, 535–545.
Fowlis, W. W., DeLucas, L. J., Twigg, P. J., Howard, S. B., Meehan, E. J. & Baird, J. K. (1988). *J. Cryst. Growth*, **90**, 117–129.
Frey, M. (1994). *Acta Cryst.* D**50**, 663–666.
Garcia-Ruiz, J. M., Moraleda, A. B., Carazo, A. & Chernov, A. (2000). In the press.
Gevorkyan, S. G. & Morozov, V. N. (1983). *Biophysics*, **28**, 1002–1007.
Huxley, H. E. & Kendrew, J. C. (1953). *Acta Cryst.* **6**, 76–80.
Izumi, K., Sawamura, S. & Ataka, M. (1996). *J. Cryst. Growth*, **168**, 106–111.
Kachalova, G. S., Morozov, V. N., Morozova, T. Y., Myachin, E. T., Vagin, A. A., Strokopytov, B. V. & Nekrasov, Y. V. (1991). *FEBS Lett.* **284**, 91–94.
Khatchaturyan, A. G. (1977). *Zh. Eksp. Teor. Fiz.* **72**, 1149–1155 (*Sov. Phys. JETP*, **45**, 601–604).
Kodandapani, R., Suresh, Ch. G. & Vijayan, M. (1990). *J. Biol. Chem.* **265**, 16126–16131.
Morozov, V. N., Kachalova, G. S., Evtodienko, V. U., Lanina, N. F. & Morozova, T. Ya. (1995). *Eur. Biophys. J.* **24**, 93–98.
Morozov, V. N. & Morozova, T. Ya. (1981). *Biopolymers*, **20**, 451–467.
Morozov, V. N., Morozova, T. Ya., Kachalova, G. S. & Myachin, G. S. (1988). *Int. J. Biol. Macromol.* **10**, 329–336.
Morozov, V. N., Morozova, T. Ya., Myachin, E. T. & Kachalova, G. S. (1985). *Acta Cryst.* B**41**, 202–205.
Nadarajah, A. & Pusey, M. L. (1996). *Acta Cryst.* D**52**, 983–996.
Nagendra, H. G., Sukumar, N. & Vijayan, M. (1998). *Proteins*, **32**, 229–240.
Otalora, F., Garcia-Ruiz, J.-M., Gavira, J.-A. & Capelle, B. (1999). *J. Cryst. Growth*, **196**, 546–558.
Perutz, M. F. (1946). *Trans. Faraday Soc. B*, **42**, 187–194.
Perutz, M. F. (1954). *Proc. R. Soc. London Ser. A*, **225**, 264–286.
Rockland, L. B. (1960). *Anal. Chem.* **32**, 1375–1376.
Rupley, J. A. & Careri, G. (1991). *Adv. Protein Chem.* **41**, 37–171.
Salunke, D. M., Veerapandian, B., Kodandapani, R. & Vijayan, M. (1985). *Acta Cryst.* B**41**, 431–436 (1985).
Stojanoff, V. & Siddons, D. P. (1996). *Acta Cryst.* A**52**, 498–499.
Stojanoff, V., Siddons, D. P., Monaco, L. A., Vekilov, P. & Rosenberger, F. (1997). *Acta Cryst.* D**53**, 588–595.
Tanner, B. K. (1976). *X-ray Diffraction Topography*. Oxford: Pergamon Press.
Vidal, O., Robert, M.-C., Capelle, B. & Arnoux, B. (1999). *J. Cryst. Growth*, **196**, 559–571.